

Indian Journal of Chemistry
Vol. 56A, May 2017, pp. 469-478

DFT studies on role of methoxy group in radical scavenging ability of quebrachitol and viscumitol

D Jeevitha^a, K Sadasivam^{a,*} & R Praveena^b

^aDepartment of Physics, Bannari Amman Institute of Technology (Autonomous), Sathyamangalam,

^bDepartment of Chemistry, Bannari Amman Institute of Technology (Autonomous), Sathyamangalam,
Erode 638 401, Tamil Nadu, India

Email: dftsada@gmail.com

Received 24 February 2017; revised and accepted 19 April 2017

The structure of quebrachitol and the influence of methoxy group on its radical scavenging ability is investigated by DFT studies. To study its electron donating ability, bond dissociation enthalpy (O-H BDE), frontier molecular orbitals (FMOs), molecular electrostatic potential (MEP) and molecular descriptors of quebrachitol and viscumitol are computed and compared. Charge delocalization and stability of the compounds are analyzed by natural bond orbital (NBO) method. The 4-OH radical of quebrachitol and 3-OH radical of viscumitol possess the least BDE and exhibit weak intramolecular hydrogen bonds which are clearly illustrated by NBO. The results show that quebrachitol, which has one methoxy group, can act as better radical scavenger than viscumitol having two methoxy groups at the same ring. The fundamental vibrational modes and wave numbers of quebrachitol are characterized theoretically based on potential energy distribution.

Keywords: Theoretical chemistry, Density functional calculations, Natural bond orbitals, Potential energy distribution, Radical scavenging, Quebrachitol, Viscumitol

Quebrachitol (6-methoxy cyclohexane-1,2,3,4,5-pentol) is a plant derived optically active cyclitol and its unique and chiral structure involved in diverse applications makes it beneficial in the pharmaceutical industry and medical research field. Quebrachitol having sweetening properties half of that of sucrose¹ is recognized as a sugar substitute for diabetics. Several studies on its use in the synthesis of optically active²⁻⁷ and bioactive natural products⁸ have been reported. Interestingly, quebrachitol plays an important role in the synthesis of L-inositol, which is used for the production of antibiotics and anticancer drugs⁹. Quebrachitol exhibits potent platelet activating factor (PAF) receptor binding inhibitory activity to rabbit platelets.¹⁰ The free radical scavenging ability of quebrachitol have been explored using DPPH assays¹¹

Quebrachitol is reported for its neuroprotective effect and its cytoprotective role is demonstrated against (6-OHDA)-initiated cell death in rat mesencephalic cell cultures *in vitro*¹². This trait makes it very effective radical scavenger. Further, quebrachitol exerts gastroprotection against gastric damage caused by ethanol and indomethacin¹³. It is an effective preservative¹⁴ for protein storage and enhances structural and thermal stabilities of proteins. The aforesaid literature of quebrachitol provides unambiguous evidence for the remarkable spectrum of biological activities and health benefits.

Structure of quebrachitol has the benzenehexol nucleus in conjugation with methoxylation at the 6-position. To explore the radical scavenging ability of quebrachitol, its electronic properties are compared with that of the compound viscumitol, which has the benzenehexol nucleus with two methoxy groups attached at 5- and 6-positions. Structures of the compounds are provided in Fig. 1. The computational characteristics of quebrachitol with one methoxy group are compared with viscumitol which has two methoxy groups and the impact of methoxylation and its biological benefits are investigated in this work.

Information on the electronic properties is essential to understand the relationship between molecular structure and the related biological activity of a compound. In the present study geometry, BDE,

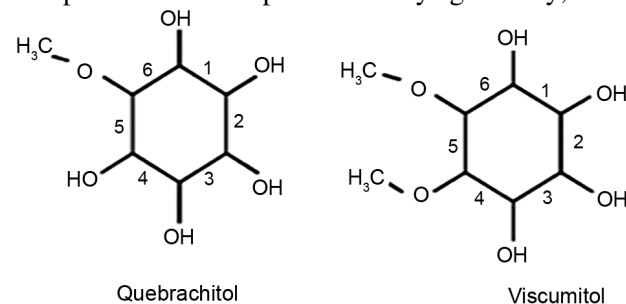


Fig. 1 – Structures and atom numbering of quebrachitol and viscumitol.

MEP, highest occupied molecular orbital (HOMO), lowest unoccupied molecular orbital (LUMO) and NBO of quebrachitol and viscumitol are analyzed and compared to understand the structural characteristics and electron donating capability of the compounds. Ionization potential (IP) and various electronic properties such as electron affinity (EA), hardness (η), softness (S), electronegativity (χ) and electrophilic index (ω) are also evaluated. In addition the vibrational spectra of quebrachitol are simulated and analyzed based on the potential energy distribution (PED) of each vibrational mode.

Computational Details

DFT calculations were performed with the Gaussian03 package¹⁵ and the molecular structures analyzed with the aid of the GaussView program¹⁶. B3LYP a hybrid functional in DFT method comprising the Becke's three parameter exchange functional B3 together with Lee-Yang-Parr correlation functional (LYP)¹⁷⁻¹⁹ was utilized. The basis set 6-311G with (d,p) polarization functions on heavy and hydrogen atoms^{20,21} were used and gas phase computations were carried out at room temperature.

IP values, i.e., the energy difference between cation radical and neutral compound, ($IP_E = E_{\text{cation}} - E_n$, $IP_O = -E_{\text{HOMO}}$). EA values (calculated as the energy difference between the neutral compound and anion radical; $EA_E = E_n - E_{\text{anion}}$; $EA_O = -E_{\text{LUMO}}$) were calculated molecular descriptors were computed using E_o (orbital energy) and E_v (total energies) of the compound. From the values of ionization potential (IP) and electron affinities (EA) the other parameters hardness, softness, electronegativity and electrophilic index were computed²² using the following equations

$$\text{Electronegativity } \chi: \mu \approx -\chi - \frac{IP + EA}{2} \quad \dots (1)$$

$$\text{Hardness } \eta \approx \frac{IP - EA}{2} \quad \dots (2)$$

$$\text{Softness } S = \frac{1}{2\eta} \quad \dots (3)$$

$$\text{Electrophilic index } \omega = \frac{\mu^2}{2\eta} \quad \dots (4)$$

PED among symmetry coordinates for quebrachitol^{23,24} was calculated. The vibrational assignments of the normal modes were computed theoretically on the basis of PED using GAR2PED program²⁵.

Results and Discussion

Molecular descriptors

To characterize the stability and activities of the compound it is vital to analyze the molecular descriptors. Each descriptor for quebrachitol and viscumitol was obtained from both total energies, E_v (generated from optimization energy) and E_o (obtained from FMO) using Koopmans' theorem²⁶ (Table 1).

IP value of quebrachitol obtained from the E_o is less than that obtained by E_v by 1.38 eV. Viscumitol is structurally similar to quebrachitol except that it has one methoxy group in excess at 5- position. IP of viscumitol obtained from E_o is less than that obtained by E_v by 1.15 eV. It is found that, IP value of quebrachitol is less by 0.18 eV (E_v) and 0.41 eV (E_o) than the IP value of viscumitol. This implies that quebrachitol can donate more electron easily than viscumitol and favors the radical scavenging ability of quebrachitol. Interestingly, it is observed that the magnitude of η for quebrachitol is lower by 0.11 eV (E_v) and 0.22 eV (E_o) than the values of viscumitol, indicating that quebrachitol is a more efficient charge transfer system than viscumitol. Domingo *et al.*²⁷ reported that a compound with $\omega > 1.5$ eV is a strong electrophile. Based on this quebrachitol is considered to be a good electrophile in both E_v and E_o methods. The same type of behavior is also observed in EA values, where quebrachitol has higher value than viscumitol, indicating that it does not accept electrons easily which is an important characteristic for a compound to be a good radical scavenger. Hence, quebrachitol is a more predominant electron donor than viscumitol. In other words, compound with one methoxy group at benzenehexol ring (quebrachitol) is a better radical scavenger than compound with two methoxy groups at the same ring (viscumitol).

The methoxy group shows significant influence on the molecular descriptors of the studied compounds. The methoxy substituent not only increases the

Table 1 – Molecular descriptors obtained at B3LYP/6-311G(d,p) level of theory

Molecular descriptors	Quebrachitol		Viscumitol	
	E_v (eV)	E_o (eV)	E_v (eV)	E_o (eV)
Ionization potential	6.72	5.34	6.90	5.75
Electron affinity	0.15	0.20	0.09	0.16
Hardness	3.29	2.57	3.40	2.79
Softness	1.65	1.28	1.70	1.39
Electronegativity	3.44	2.77	3.49	2.95
Electrophilic index	1.80	1.55	1.79	1.49

magnitude of IP but also increases the HOMO-LUMO band gap. Further, χ , η and S of the compound indicate that the presence of two methoxy group decreases the reactivity of viscumitol. Hence, it is concluded from the results that radical scavenging ability increases with decreasing order of methoxy group.

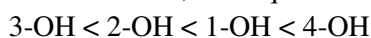
Bond dissociation enthalpy

The OH-BDE parameter, connected to the H-atom or a single electron transfer pathway, is of specific importance to the mechanism of radical scavenging activity²⁸. The computed BDE values for quebrachitol and viscumitol compounds are shown in Table 2. In quebrachitol, the formation of the 4-OH radical (70.12 kcal/mol) radical is easier than other radicals. The radicalization of 5-OH (74.66 kcal/mol) needs higher energy for the release of H-atom transfer. For viscumitol, the H-abstraction is predominant at 3-OH (72.14 kcal/mol) and is weak at 4-OH group (75.06 kcal/mol). The 4-OH for quebrachitol and 3-OH for viscumitol are the most favoured deprotonation sites because of their enhanced possibility to delocalize the electron pair. This is clearly demonstrated by the NBO analysis. Quebrachitol bearing one methoxy group on 6-position presented lower BDE value, in comparison to viscumitol, having two methoxy groups on 5- and 6-positions.

Thus, the order of preference of the position from which a hydrogen atom is most likely to be abstracted in quebrachitol is:



For viscumitol, the sequence is as follows:



When the magnitude of BDE quebrachitol is considered, the 1-OH radical is lower by 1.35 kcal/mol, 2-OH is lower by 1.74 kcal/mol, 3-OH is higher by 0.27 kcal/mol and 4-OH group is lower by 4.94 kcal/mol as compared to the values of

viscumitol. This clearly confirms that H-atom transfer is easier from quebrachitol and it exhibits better radical scavenging ability than viscumitol. Considering the molecular structure of quebrachitol, the better activity as radical scavenger can be ascribed to the penta-hydroxyl group of quebrachitol. Presence of methoxy group governs the BDE; existence of two methoxy groups in viscumitol decreases its reactivity. It is interesting to note that electron donating ability of a compound generally associated with the number of O-H groups and methoxy groups in it. It is found that the radical scavenging ability increases with increasing number of O-H groups and decreasing number of methoxy groups. Also, a compound with a methoxy group in the benzenehexol ring (quebrachitol) is a better radical scavenger than a compound with two methoxy groups in the same ring (viscumitol). Hence, quebrachitol is a better radical scavenger than viscumitol.

Molecular electrostatic potential

MEP is an important parameter providing information regarding the molecular properties of small and drug molecules. The appropriate regions for the electrophilic and nucleophilic attacks can be visualized by a MEP map²⁹. The electron density rich area is represented by red while the poor electron density is indicated by blue surface. The increasing order of electron density is given under red < orange < yellow < green < blue.

The MEP plots of quebrachitol and viscumitol depicted in Fig. 2 reveal the presence of oxygen atoms on the hydroxyl group of the rings (characterized by red color) and are considered to be the most negative potential region. The presence of hydrogen atoms in the hydroxyl group are symbolized by blue regions bearing the positive charge.

For quebrachitol, the color code of MEP surface varies from deepest red (-0.04618 a.u.) to deepest blue (0.04618 a.u.). The most probable site for electrophilic attack over oxygen atoms are at 1-OH, 2-OH, 3-OH, 4-OH, 5-OH and -OCH₃ groups. High electrophilic reactivity observed from the concentration of electrons over the oxygen atom and weaker electron population on hydrogen atom indicates nucleophilic attack. The predominant electron density on the methoxy group indicates the electron withdrawing nature of methoxy group due the inductive effect of oxygen atom. For viscumitol, the color code of MEP surface varies from deepest red (-0.04703 a.u. to deepest blue (0.04703 a.u.). The

Table 2 – Calculated bond dissociation enthalpy values (BDE) at 298.15 K in the gas phase for quebrachitol and viscumitol, at the B3LYP/6-311G(d,p) level of theory

Radicals	BDE (kcal/mol)	
	Quebrachitol	Viscumitol
1-OH	72.66	74.01
2-OH	70.66	72.40
3-OH	72.41	72.14
4-OH	70.12	75.06
5-OH	74.66	-

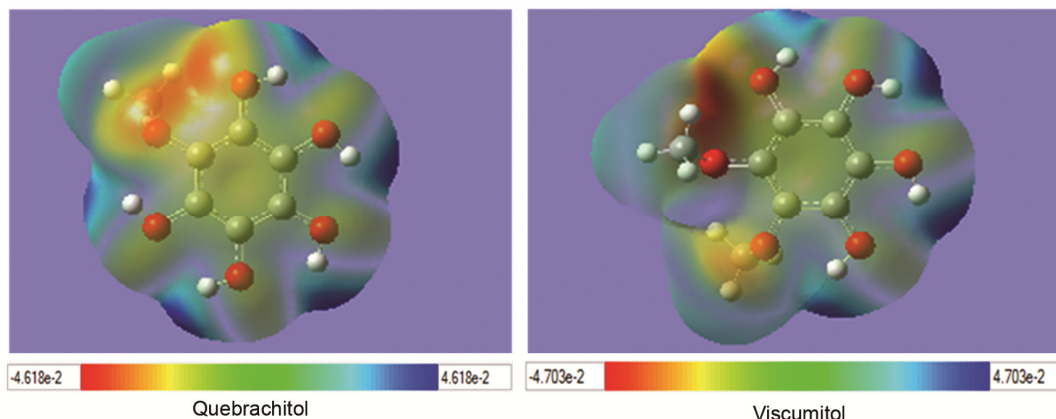


Fig. 2 – MEP plot of quebrachitol and viscumitol using B3LYP/6-311(d,p) by DFT model chemistry.

most probable region for electrophilic attack is spread over all the oxygen atoms of the functional groups (1-OH, 2-OH, 3-OH, 4-OH and -OCH₃); the methoxy group registers the highest electrophilic index.

Frontier molecular orbital

In order to evaluate the electronic transitions of the title compounds, in addition to the HOMO, LUMO, the second highest MO's (HOMO-1), the second lowest unoccupied MO' (LUMO+1) were analyzed. As shown in Fig. 3(a) and 3(b), the basic skeleton contains high charge concentration as compared to the rest of the molecule. On analyzing the HOMO orbital of quebrachitol, the charge localization is found to be maximum on the O-H groups and the benzene ring. Absence of charge localization on the methoxy group is due to the steric hindrance. On excluding the methoxy group, the LUMO and LUMO+1 orbitals show spread of the electron cloud over the entire region, whereas the same behaviour is observed in HOMO-1 orbital with inclusion of the methoxy group.

The electronic structure of viscumitol exhibits prominent charge density concentration on O-H groups and benzene ring. Poor charge distribution is witnessed on HOMO and HOMO-1 orbitals, while the LUMO orbital is characterized by high charge density dispersed over the entire compound. Similarly, LUMO+1 shows high charge density distribution on the entire compound with small concentration of charge on the methoxy groups.

Stronger radical scavenging activity of quebrachitol as compared to viscumitol, is evidenced from the computed HOMO magnitudes (Table 3). Energy separation between HOMO-LUMO of quebrachitol is obtained as 5.14 eV, whereas it is 5.59 eV for

Table 3 – Frontier orbital energies and band gap energies of quebrachitol and viscumitol

	Quebrachitol	Viscumitol
- ϵ_{HOMO} (eV)	5.34	5.75
- ϵ_{LUMO} (eV)	0.20	0.16
Energy gap (eV)	5.14	5.59

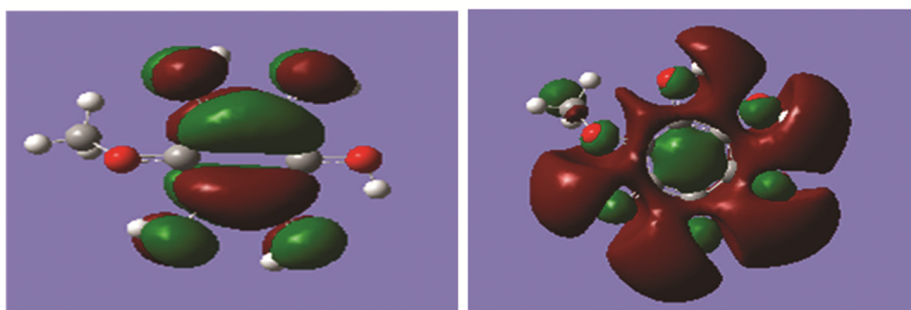
viscumitol. Lower energy gap is related to the stronger electron donation and more vigorous radical scavenging activity which implies quebrachitol is the better electron donor. According to the HOMO and energy gap values, it is very clear that one methoxy group attached with benzenehexol ring (quebrachitol) is a better radical scavenger than two methoxy groups attached at the same ring (viscumitol). Inclusion of methoxy group affects the electron donating ability which agrees with the molecular descriptors and BDE results.

Natural bond analysis

NBO analysis³⁰ gives information about intramolecular bonding and interactions among bonds and is implemented for investigating charge transfer or conjugative interaction in the molecule³¹. The second order perturbation theory was applied to analyze donor-acceptor interactions in the NBO method³². NBO analysis was performed on quebrachitol and viscumitol using NBO 3.1 program in the Gaussian03W package at the DFT-B3LYP/6-311G(d,p) level of theory and hyperconjugative interaction energy value was obtained from the second-order perturbation theory³³. The interacting stabilization energy $E(2)$ was computed for each donor (i) and acceptor (j) as follows:

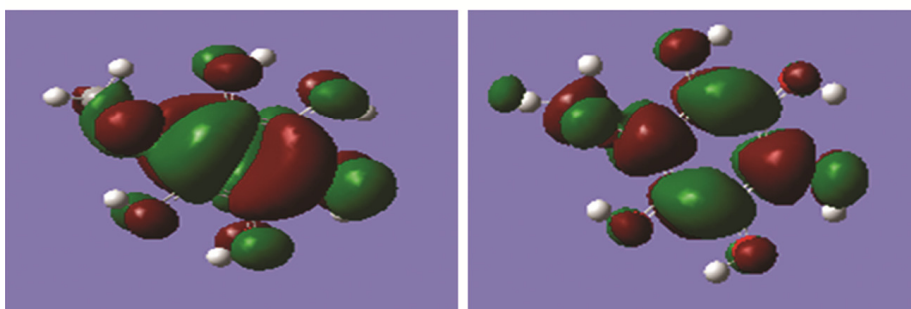
$$E_2 = \Delta E_{ij} = q_i \frac{F(i,j)^2}{\epsilon_i - \epsilon_j}, \text{ where } q_i \text{ is donor orbital occupancy,}$$

Quebrachitol



HOMO

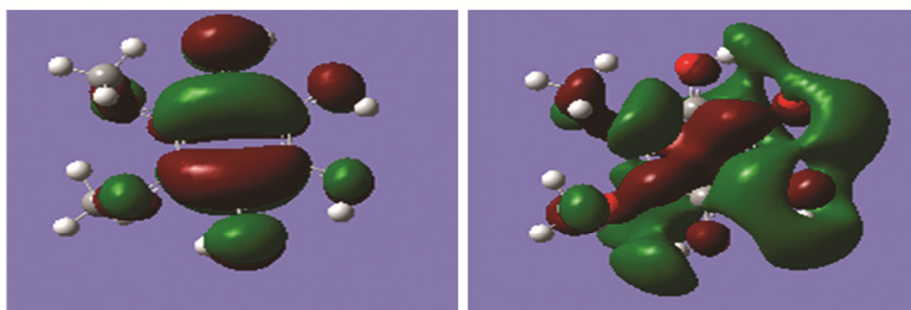
LUMO



HOMO-1

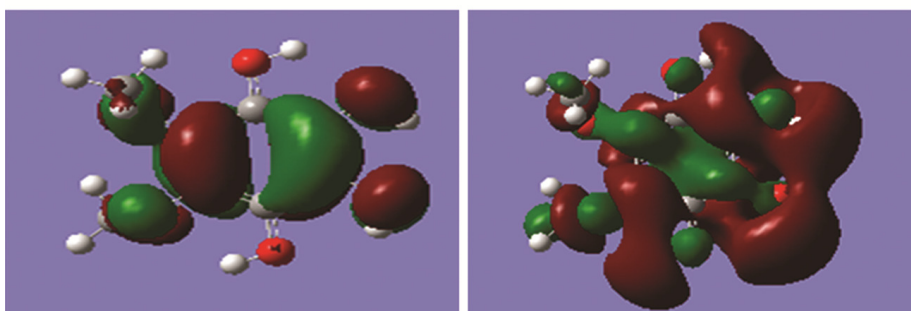
LUMO+1

Viscumitol



HOMO

LUMO



HOMO-1

LUMO+1

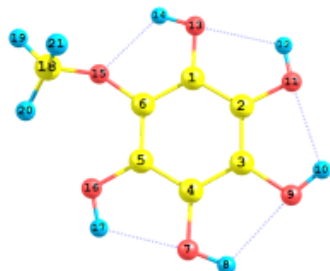
Fig. 3 – Frontier molecular orbital distribution for quebrachitol and viscumitol.

ϵ_i and ϵ_j are diagonal elements and $F(i,j)$ is the off diagonal Fock matrix element reported^{34,35}. Higher value of $E(2)$ implies stronger hyperconjugative interaction between electron donors and acceptors (Table 4).

The hyperconjugative interactions from the aromatic ring carbon atoms for quebrachitol are C1-C2→C3-C4 (20.59 kcal/mol), C3-C4→C5-C6 (20.20 kcal/mol) and C5-C6→C1-C2 (20.98 kcal/mol).

Table 4 – Second order perturbation theory analysis of Fock matrix for NBO analysis for quebrachitol and viscumitol

Donor (i) Acceptor (j) $E(2)$ (kcal/mol) $E(j)-E(i)$ (a.u.) $F(i,j)$ (a.u.)

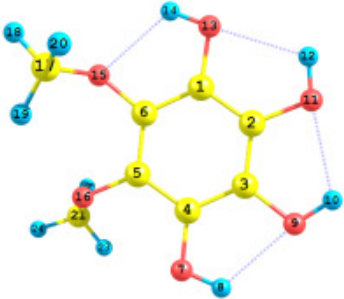


Quebrachitol

$\pi(C1-C2)$	$\pi^*(C2-O11)$	0.59	1.05	0.022
	$\pi^*(C3-O9)$	3.49	1.05	0.054
	$\pi^*(O13-H14)$	1.26	1.12	0.034
$\sigma(C1-C2)$	$\sigma^*(C3-C4)$	20.59	0.29	0.072
	$\sigma^*(C5-C6)$	17.60	0.29	0.067
$\pi(C1-C6)$	$\pi^*(C1-O13)$	0.51	1.05	0.021
	$\pi^*(C6-O15)$	0.65	1.05	0.023
	$\pi^*(O15-C18)$	2.03	0.98	0.040
$\pi(C1-O13)$	$\pi^*(C1-C2)$	0.94	1.46	0.033
	$\pi^*(C5-C6)$	1.55	1.45	0.043
$\pi(C2-C3)$	$\pi^*(C1-O13)$	3.09	1.06	0.051
	$\pi^*(C2-O11)$	0.69	1.05	0.024
	$\pi^*(C3-O9)$	0.51	1.05	0.021
	$\pi^*(C4-O7)$	3.40	1.05	0.053
	$\pi^*(O11-H12)$	1.27	1.12	0.034
$\pi(C2-O11)$	$\pi^*(C1-C2)$	1.37	1.45	0.040
$\pi(C3-C4)$	$\pi^*(C3-O9)$	0.72	1.05	0.025
	$\pi^*(C5-O16)$	2.92	1.06	0.050
	$\pi^*(O9-H10)$	1.30	1.12	0.034
	$\sigma^*(C1-C2)$	18.03	0.29	0.068
$\sigma(C3-C4)$	$\sigma^*(C5-C6)$	20.20	0.29	0.072
	$\pi^*(C1-C2)$	1.44	1.46	0.041
$\pi(C3-O9)$	$\pi^*(C4-C5)$	1.78	1.45	0.046
	$\pi^*(C3-O9)$	2.96	1.05	0.050
$\pi(C4-C5)$	$\pi^*(C6-O15)$	4.15	1.06	0.059
	$\pi^*(O7-H8)$	1.30	1.12	0.034
	$\pi^*(C1-O13)$	3.12	1.05	0.051
$\pi(C5-C6)$	$\pi^*(O15-C18)$	0.63	0.98	0.022
	$\pi^*(O16-H17)$	1.19	1.12	0.033
	$\sigma^*(C1-C2)$	20.98	0.29	0.073
$\sigma(C5-C6)$	$\sigma^*(C3-C4)$	17.92	0.29	0.067
	$\pi^*(C18-H19)$	0.50	0.66	0.018
	$\pi^*(C3-C4)$	1.57	1.45	0.043
$\pi(C5-O16)$	$\pi^*(C1-C2)$	1.87	1.43	0.046
$\pi(C6-O15)$	$\pi^*(C4-C5)$	4.06	1.29	0.065

(Contd.)

Table 4 – Second order perturbation theory analysis of Fock matrix for NBO analysis for quebrachitol and viscumitol (*Contd.*)

Donor (i)	Acceptor (j)	$E(2)$ (kcal/mol)	$E(j)-E(i)$ (a.u.)	$F(i,j)$ (a.u.)
Quebrachitol				
$\pi(O9-H10)$	$\pi^*(C3-C4)$	4.20	1.30	0.066
$\pi(O11-H12)$	$\pi^*(C2-C3)$	4.18	1.29	0.066
$\pi(O13-H14)$	$\pi^*(C1-C2)$	4.40	1.29	0.068
$\pi(O15-C18)$	$\pi^*(C1-C6)$	1.42	1.34	0.039
$\pi(O16-H17)$	$\pi^*(C5-C6)$	4.65	1.28	0.069
$\pi(C18-H20)$	$\pi^*(C6-O15)$	0.54	0.87	0.019
$\pi(C18-H21)$	$\pi^*(C6-O15)$	0.57	0.87	0.020
	$\pi^*(O15-C18)$	0.52	0.80	0.018
LP(1)O7	$\pi^*(C3-C4)$	5.99	1.17	0.075
	$\pi^*(O16-H17)$	0.78	1.03	0.025
LP(2)O7	$\sigma^*(C3-C4)$	23.01	0.35	0.089
LP(2)O9	$\sigma^*(C3-C4)$	23.76	0.35	0.090
LP(2)O11	$\sigma^*(C1-C2)$	23.04	0.35	0.089
LP(2)O13	$\sigma^*(C1-C2)$	24.22	0.35	0.091
LP(1)O15	$\pi^*(O13-H14)$	0.75	0.96	0.024
	$\pi^*(C18-H19)$	2.49	0.95	0.044
	$\pi^*(C18-H20)$	1.13	0.96	0.030
LP(2)O15	$\pi^*(O13-H14)$	0.90	0.73	0.023
	$\pi^*(C18-H20)$	4.36	0.73	0.051
LP(2)O16	$\sigma^*(C5-C6)$	26.46	0.34	0.094
				
Viscumitol				
$\pi(C1-C2)$	$\pi^*(C1-O13)$	0.66	1.05	0.024
	$\pi^*(O13-H14)$	1.25	1.12	0.033
$\pi(C1-C6)$	$\pi^*(C1-C2)$	4.89	1.26	0.070
	$\pi^*(C2-O11)$	3.55	1.04	0.054
	$\pi^*(O15-C17)$	1.87	0.98	0.038
$\sigma(C1-C6)$	$\sigma^*(C4-C5)$	18.54	0.29	0.069
	$\pi^*(O15-C17)$	1.86	0.54	0.031
$\pi(C1-O13)$	$\pi^*(C1-C2)$	0.92	1.45	0.033
	$\pi^*(C5-C6)$	1.56	1.45	0.043
$\pi(C2-C3)$	$\pi^*(C1-C2)$	4.51	1.27	0.068
	$\pi^*(C1-O13)$	3.09	1.06	0.051
	$\pi^*(O11-H12)$	1.29	1.12	0.034
$\sigma(C2-C3)$	$\sigma^*(C1-C6)$	19.75	0.30	0.071
$\pi(C2-O11)$	$\pi^*(C1-C2)$	1.33	1.46	0.040
$\pi(C3-C4)$	$\pi^*(C2-C3)$	4.45	1.26	0.067

(Contd.)

Table 4 – Second order perturbation theory analysis of Fock matrix for NBO analysis for quebrachitol and viscumitol (*Contd*)

Donor (i)	Acceptor (j)	$E(2)$ (kcal/mol)	$E(j)-E(i)$ (a.u.)	$F(i,j)$ (a.u.)
		Viscumitol		
$\pi(C4-C5)$	$\pi^*(C3-C4)$	4.19	1.25	0.065
	$\pi^*(C4-O7)$	0.94	1.05	0.028
	$\pi^*(O7-H8)$	1.19	1.12	0.033
	$\pi^*(O16-C21)$	0.75	0.99	0.024
$\sigma(C4-C5)$	$\pi^*(C21-H24)$	0.56	0.67	0.019
$\pi(C4-O7)$	$\pi^*(C2-C3)$	1.59	1.45	0.043
$\pi(C5-C6)$	$\pi^*(C1-C6)$	4.39	1.26	0.066
	$\pi^*(C1-O13)$	3.24	1.04	0.052
	$\pi^*(C4-C5)$	3.82	1.25	0.062
$\pi(C5-O16)$	$\pi^*(C4-C5)$	1.15	1.42	0.036
	$\pi^*(C5-C6)$	1.16	1.42	0.037
$\pi(C6-O15)$	$\pi^*(C1-C2)$	1.87	1.42	0.046
	$\pi^*(C1-C6)$	0.84	1.42	0.031
$\pi(O7-H8)$	$\pi^*(C4-C5)$	4.57	1.28	0.069
$\pi(O9-H10)$	$\pi^*(C3-C4)$	4.11	1.29	0.065
$\pi(O15-C17)$	$\pi^*(C1-C6)$	1.26	1.35	0.037
$\pi(O16-C21)$	$\sigma^*(C4-C5)$	2.29	0.81	0.044
$\pi(C17-H18)$	$\pi^*(C6-O15)$	3.77	0.87	0.051
$\pi(C17-H20)$	$\pi^*(C6-O15)$	0.62	0.87	0.021
	$\pi^*(O15-C17)$	0.51	0.80	0.018
LP(1)O7	$\pi^*(C3-C4)$	5.93	1.15	0.074
LP(1)O9	$\pi^*(C2-C3)$	6.00	1.17	0.075
	$\pi^*(O7-H8)$	0.76	1.03	0.025
LP(1)O15	$\pi^*(C5-C6)$	4.63	1.11	0.064
	$\pi^*(O13-H14)$	0.66	0.96	0.023
	$\pi^*(C17-H18)$	2.40	0.95	0.043
LP(2)O15	$\sigma^*(C1-C6)$	6.67	0.35	0.048
	$\pi^*(O13-H14)$	0.88	0.73	0.023
LP(2)O16	$\pi^*(C21-H22)$	5.86	0.73	0.059
$\sigma^*(C1-C6)$	$\pi^*(O15-C17)$	1.08	0.25	0.030

For viscumitol, there are C1-C6→C4-C5 (18.54 kcal/mol), C2-C3→C1-C6 (19.75 kcal/mol). Strong stabilization energies between the aromatic ring carbon atoms shows the stability of the compound and also lead to extending the electron delocalization over the entire molecular system.

The interactions C1-C6→C1-O13 (0.51 kcal/mol), C5-O16→C3-C4 (1.57 kcal/mol), C18-H21→O15-C18 (0.52 kcal/mol) and C18-H20→C16-O15 (0.54 kcal/mol) of quebrachitol and the interactions C1-C2→C1-O13 (0.66 kcal/mol), C6-O15→C1-C6 (0.84 kcal/mol) and C17-H20→O15-C17 (0.51 kcal/mol) of viscumitol contribute to poor stabilization energy.

The hyperconjugative interaction is more intensive from (O-H) to (C-C) orbital than from (C-C) to (O-H) orbital. Magnitude of charges transferred from O9-H10→C3-C4 (4.20 kcal/mol) and O16-H17→C5-C6 (4.65 kcal/mol) of quebrachitol are considerably larger than from C1-C2→O13-H14 (1.26 kcal/mol)

and C5-C6→O16-H17 (1.19 kcal/mol). Also, magnitudes of the interactions, O9-H10→C3-C4 (4.11 kcal/mol) and O7-H8→C4-C5 (4.57 kcal/mol) of viscumitol are slightly larger than C4-C5→O7-H8 (1.19 kcal/mol) and C1-C2→O13-H14 (1.25 kcal/mol).

The interaction energy, related to the resonance in the compound, are the charge transfer from lone pairs of oxygen to O-H anti-bonding orbital. For quebrachitol, LP(1)O7→O16-H17(0.78 kcal/mol) afford weak intramolecular interaction. It is obvious from BDE results that the radical 4-OH of quebrachitol has lowest BDE which is due to the weak intramolecular hydrogen bond existing at LP(1)O7→O16-H17. In the case of viscumitol, LP(1)O9→O7-H8 (0.76 kcal/mol) affords weak intramolecular interaction, leading to the 3-OH radical of the viscumitol having least BDE. These types of molecular interactions are useful for the structure-activity relationships relevant to radical scavenging ability.

Vibrational assignments

The total number of atoms in the quebrachitol molecule is 21 resulting in 57 (3N-6) normal modes. Vibrational analysis of the 57 fundamental normal modes of the quebrachitol is reported on the basis of DFT/6-311G(d,p) quantum chemical calculations. The assigned scaled wave numbers (by WLS scale factor) of the compound along with the PED for each normal mode are given in Table S1 (Supplementary Data). The assignments are reported on the basis of internal coordinate system recommended by Pulay *et al.*²³ with the localized symmetry used for analyzing PED using the program GAR2PED³⁶. PED values <5% have been excluded in the table. Scaled simulated spectra of quebrachitol is illustrated in Fig. 4.

In quebrachitol, ring vibrations are a major contribution in the simulated spectrum of the sample. In the present study, the calculations yielded the C-C stretching vibrations at 1658, 1638, 1523, 1506, 1439, 1374 and 1192 cm^{-1} . The wave numbers of the asymmetric and symmetric deformation of the ring are calculated to be 464 and 481, 284 cm^{-1} respectively. The trigonal deformation modes are generally predicted in the region of 1312-1293 cm^{-1} . The asymmetric torsion modes are found to be at 652, 620, 169 and 115 cm^{-1} . The wave numbers at 682, 620, 257 and 182 cm^{-1} are attributed to puckering modes.

Quebrachitol possesses one methoxy group substituted in the sixth position. The $-\text{CH}_3$ group gives rise to nine internal modes of vibrations, i.e., one each of symmetric stretching, asymmetric stretching and antisymmetric deformation, symmetric bending, in-plane rocking, out-of-plane rocking and torsion mode and two each of the $-\text{CH}_3$ symmetric and antisymmetric stretching vibrations generally lie at the lower frequency region 2850-3000 cm^{-1} ³⁷. For the title compound, peaks identified at 2896, 2973 and 3002 cm^{-1} are ascribed to symmetric and antisymmetric stretching vibration. It is obvious from the PED column that these are pure stretching modes and contribute 100%.

For methoxy substituted benzene derivatives, the vibrations of antisymmetric deformation³⁷ appears in the region 1465-1440 cm^{-1} and for quebrachitol it is calculated to be at 1461 and 1488 cm^{-1} . Rocking frequencies produced by methoxy group are variable in position due to interactions with skeleton stretching modes. The computed wave numbers for these vibrations are at 1160, 1192 and 1199 cm^{-1} . The

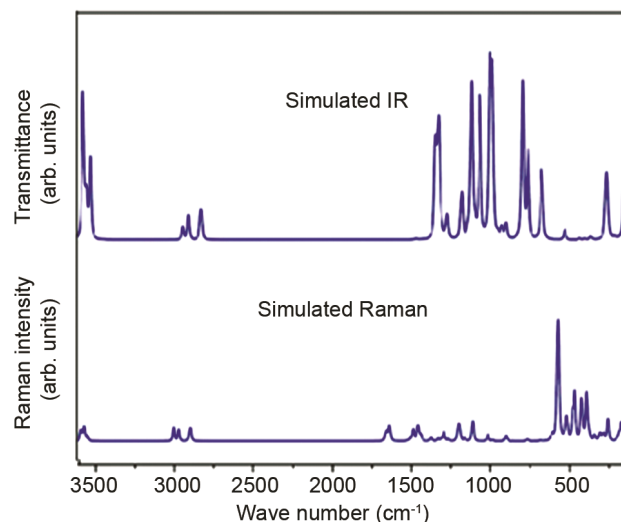


Fig. 4 – Simulated IR and Raman spectra of quebrachitol.

calculated wave numbers for $\omega(\text{OC})$ wagging mode are 73 and 115 cm^{-1} . The frequency of $-\text{CH}_3$ torsional mode is expected below 400 cm^{-1} , and the computed band at 169 and 182 cm^{-1} is assigned to this mode³⁸.

The compound contains five O-H groups connected to the ring. In the simulated spectrum of quebrachitol (Fig. 4), the characteristic peak corresponding to the stretching mode of the OH group is identified at 3590, 3587, 3580, 3567 and 3548 cm^{-1} and the PED corresponding to this mode contributes almost 100%. The stretching frequencies due to C-O band³⁹ appear in spectrum at 902, 986, 1111 and 1136 cm^{-1} . The scaled vibrational modes computed in the range 284-341 cm^{-1} , correspond to the CCO in-plane bending vibrations and the modes calculated at 1199, 1211, 1266, 1293 and 1332 cm^{-1} are assigned to the OH bending vibrations. The wave numbers 200, 257, 374, 652 and 682 cm^{-1} are ascribed to C-O out-of-plane bending.

Conclusions

DFT studies on electron donating ability of quebrachitol and viscumitol reveal that quebrachitol (benzenehexol with one methoxy group) has higher IP and EA values as compared to viscumitol (benzenehexol with two methoxy groups). It is evident from the simulation studies that the presence of methoxy substituent also increases the HOMO-LUMO energy gap by 0.45 eV. Our results indicate that 4-OH of quebrachitol and 3-OH of viscumitol are the most favored sites for O-H bond breaking, exhibiting the lowest BDE values. This is also

evidenced by NBO analysis of quebrachitol and viscumitol. MEP surface plots have been studied to map out the efficient H-donor system. The most probable site for potential scavenging activity is found to be the 4-OH of quebrachitol and 3-OH of viscumitol. Frequency assignments for normal modes of vibrations for quebrachitol have been done using FT-IR and compared with the available literature on experimental analysis. In general, a good agreement between experimental and theoretical calculations was observed. Based on the molecular descriptors and other characterization results, it is concluded that quebrachitol may be exploited for its electron donating ability. Also, it may be concluded that the compound with lesser number of methoxy groups (quebrachitol) is the more promising radical scavenger.

Acknowledgement

The authors are highly thankful to Dr Poonam Tanton and Dr T Karthick, University of Lucknow, India for the computation of potential energy distribution (PED).

References

- McCance R A & Lawrence R D, *Biochem J*, 27 (1933) 986.
- Angyal S J & Hoskinson R M, *Methods Carbohydr Chem*, 2 (1963) 87.
- Ogawa S & Isaka A, *Carbohydr Res*, 210 (1991) 105.
- Akiyama T, Takechi N & Ozaki S, *Tetrahedron Lett*, 31 (1990) 1433.
- Akiyama T, Shima H & Ozaki, *Tetrahedron Lett*, 32 (1991) 5593.
- Chida N, Tobe T & Ogawa S, *Tetrahedron Lett*, 32 (1991) 1063.
- Ogawa S & Isaka A, *Carbohydr Res*, 210 (1991) 105.
- Kiddle J J, *Chem Rev*, 95 (1995) 2189.
- Sanseera D, Niwatananun W, Liawruangrath B, Liawruangrath S, Baramée A, Trisuwan K & Pyne S G, *CMU J Nat Sci*, 11 (2012) 157.
- Moharam B A, Jantan I, Jalil J & Shaari K, *Molecules*, 15 (2010) 7840.
- Lemos T L G, Machado L L, Souza J S N, Fonseca A M, Maia J L & Pessoa O D L, *Fitoterapia*, 77 (2006) 443.
- Junior H V N, Cunha G M A, Moraes M O, Luciana M F D, Oliveira R A, Maia F D, Nogueira M A S, Lemos T L G & Rao V S, *Food Chem Toxicol*, 44 (2006) 1544.
- Olinda T M D, Lemos T L G, Machado L L, Rao V S & Santos F A, *Phytomedicine*, 15 (2008) 327.
- Ortbauer M & Popp M, *Plant Physiol Bioch*, 46 (2008) 428-434.
- Gaussian 03W, Rev E.01*, (Gaussian, Inc., Wallingford CT) 2004.
- GAUSSVIEW User Manual*, (Gaussian Inc., Pittsburgh, PA, USA) 2000.
- Lee C T, Yang W T & Parr R G, *Phys Rev B*, 37 (1988) 785.
- Parr R G & Yang W, *Density Functional Theory of Atoms and Molecules*, Oxford University Press, New York (1989).
- Becke A D, *J Chem Phys*, 98 (1993) 5648.
- Petersson G A & Allaham M A, *J Chem Phys*, 94 (1991) 6081.
- Petersson G A, Bennett A, Tensfeldt T G, Allaham M A, Shirley W A & Mantzaris J, *J Chem Phys*, 89 (1988) 2193.
- Domingo L R, Rios-Gutierrez M & Perez P, *Molecules*, 21 (2016) 748.
- Pulay P, Fogarasi G, Pang F & Boggs J E, *J Am Chem Soc*, 101 (1979) 2550.
- Fogarasi G, Zhou X, Taylor P W & Pulay P, *J Am Chem Soc*, 114 (1992) 8191.
- Martin J M L & Van Alsenoy C, *Gar2ped*, University of Antwerp, 1995.
- Koopmans T, *Physica*, 1 (1934) 104.
- Domingo L R, Aurell M J, Perez P & Contreras R, *Tetrahedron*, 58 (2002) 4417.
- Wright J S, Johnson E R & Dilabio G A, *J Am Chem Soc*, 123 (2001) 1173.
- Tomasi J, in *Chemical Application of Atomic and Molecular Electrostatic Potentials*, edited by P Politzer & D Truhlar, (Plenum, New York) 1981, pp. 257.
- Moro S, Bacilieri M, Ferrari C & Spalluto G, *Curr Drug Discov Technol*, 2 (2005) 13.
- Murray J S & Sen K, *Molecular Electrostatic Potentials, Concepts and Applications*, (Elsevier, Amsterdam) 1996.
- Karabacak M, Sinha L, Prasad O, Cinar Z & Cinar M, *Spectrochim Acta A*, 93 (2012) 33.
- Sarafran M, Komasa A & Adamska E B, *J Mol Struct: THEOCHEM*, 827 (2007) 101.
- Glendening E D, Badenhoop J K, Reed A E, Carpenter J E, Bohmann J A, Morales C M & Weinhold F, *NBO 5.0*, (Theoretical Chemistry Institute, University of Wisconsin, Madison,) 2001.
- Na L J, Rang C Z & Fang Y S, *J Zhejiang Univ Science*, 6B (2005) 584.
- Martin J M L & Alsenoy V & Alsenoy C V, *Gar2ped*, (University of Antwerp, Antwerp) 1995.
- Prabavathi N & Senthil Nayagi N, *J Environ Nanotechnol*, 3 (2014) 108.
- Bee S, Agarwal P, Gupta A & Tandon P, *Spectrochim Acta*, 114 (2013) 236.
- Krishnakumar V & Prabavathi N, *Spectrochim Acta*, 77 (2010) 238.